УДК 621.794.61; 621.9.048.7
P.A.C.S. 81.65.Mq
DOI 10.54708/26587572_2023_5313109

INVESTIGATION ON THE PROPERTIES OF ANODIC OXIDES GROWN ON ALUMINIUM-SILICON ALLOYS IRRADIATED BY PULSED ELECTRON BEAM

Massimiliano Bestetti [1, 2a], Lucchini Huspek Andrea [1], Agdokan Batuhan [1], Yuriy Haljafovich Akhmadeev [3], Elizaveta Alekseevna Petrikova [3], Yurii Fedorovich Ivanov [3], Pavel Vladimirovich Moskvin [3], Nikolay Nikolaevich Koval [3]

[1] Polytechnic University of Milan, Leonardo da Vinci sq. 32, 20133, Milan, Italy
[2] Tomsk Polytechnic University, Weinberg Research Centre, Lenin pr. 30, 634050, Tomsk, Russia
[3] Institute of High Current Electronics, Siberian branch of the Russian Academy of Science, Akademichesky pr. 2/3, 634055, Tomsk, Russia
[a] massimiliano.bestetti@polimi.it

ABSTRACT

Al-Si alloys are among the most common aluminium based materials for cast products due to their high strength-to-weight ratio, excellent processability and relatively low cost. The presence of Si in the molten Al phase improves the castability and decreases the solidification shrinkage. Hard anodic oxidation is largely employed to improve their surface mechanical properties and corrosion resistance. However, the presence of high Si contents (> 3%) and the size of Si particles in the alloy make the process challenging or even not possible. The surface pretreatment of Al-Si alloys with intense pulsed electron beams (EB) can effectively overcome the aforementioned limitations. Electron beam sources can be employed to reduce Si content and to refine and disperse Si particles, and effectively create an Al substrate that is more prone to oxidization. In the present work, two electron beam units were used, RITM-SP and SOLO, to modify the surface properties of hypoeutectic, eutectic and hypereutectic Al-Si alloys, by investigating the effect of energy density and number of pulses. The electron beam treated substrates were hard anodized and characterized in term of microstructure, elemental distribution, corrosion resistance and surface mechanical properties.

KEYWORDS

Al-Si alloys; electron beam; hard anodizing; RITM-SP; SOLO.

ИССЛЕДОВАНИЕ СВОЙСТВ АНОДНЫХ ОКСИДОВ, ВЫРАЩЕННЫХ НА ПОВЕРХНОСТИ АЛЮМИНИЕВО-КРЕМНИЕВЫХ СПЛАВОВ, ПОДВЕРГНУТЫХ ОБЛУЧЕНИЮ ИМПУЛЬСНЫМИ ЭЛЕКТРОННЫМИ ПУЧКАМИ

Массимилиано Бестетти [1, 2a], Лучини Хуспек Андреа [1], Агдокан Батуан [1], Юрий Халяфович Ахмадеев [3], Елизавета Алексеевна Петрикова [3], Юрий Федорович Иванов [3], Павел Владимирович Москвин [3], Николай Николаевич Коваль [3]

[1] Миланский технический университет, 20133, Италия, Милан, пл. Леонардо да Винчи, 32
[2] Томский политехнический университет, Научно-образовательный центр Б. П. Вейнберга, 634050, Россия, Томск, пр. Ленина, 30
[3] Институт сильноточной электроники СО РАН, 634055, Россия, Томск, Академический пр., 2/3
[a] massimiliano.bestetti@polimi.it

АННОТАЦИЯ

Сплавы системы Al-Si являются одними из наиболее широко распространенных материалов на основе алюминия, используемых для изготовления литых изделий, благодаря своей удельной прочности, отличной обрабатываемости и относительно низкой стоимости. Наличие кремния в фазе расплавленного алюминия улучшает литейные свойства и снижает усадку при затвердевании. Для улучшения их поверхностных механических свойств и коррозионной стойкости применяется твердое анодное оксидирование. Однако наличие высокого содержания кремния (> 3%) и размер частиц Si в сплаве делают данный процесс сложным или даже невозможным. Предварительная обработка поверхности сплавов системы Al-Si интенсивными импульсными электронными пучками позволяет эффективно преодолеть вышеуказанные ограничения. Источники электронных пучков могут использоваться для снижения содержания кремния, измельчения частиц Si, а также для создания алюминиевой подложки, более предрасположенной к оксидированию. В данной работе две электронно-пучковые установки, «РИТМ-СП» и «СОЛО», использовались для изменения поверхностных свойств доэвтектических, эвтектических и заэвтектических сплавов системы Al-Si путем исследования влияния плотности энергии и числа импульсов. После обработки электронными пучками образцы подвергались твердому анодированию, и проводилась аттестация их микроструктуры, распределения элементов, коррозионной стойкости и поверхностных механических свойств.

КЛЮЧЕВЫЕ СЛОВА

Сплавы Al-Si; электронный пучок; твердое анодирование; РИТМ-СП; СОЛО.

Introduction

It is well known that Al passivates spontaneously by forming a thin (few nm) native oxide when exposed to the environment. However, in acidic or alkaline conditions the native oxide layer is not able to ensure sufficient protection from corrosion. As a consequence, anodic oxidation is primarily employed to enhance hardness and corrosion resistance. For instance, in the automotive and aerospace applications, a high mechanical and corrosion resistance is mandatory. In general, hard anodic oxidation is performed in acidic refrigerated aqueous solutions and by applying current densities of few A/dm^2. As a consequence, the formation of dense and thick protective coatings can be achieved in a relatively short processing time [1]. In the case of some aluminium alloys, the process still encounters problems related to the formation of a thick and hard enough coating, especially when dealing with highly alloyed substrates such as series 2000, 3000, 4000 and 7000 [2]. The presence of alloying elements in large amounts can alter the characteristics of the oxide layer. Among the different Al foundry alloys, Al-Si are of particular interest when dealing with anodic oxidation. In fact, the presence of silicon, eutectic structures and other intermetallic phases drastically modify the final characteristics of the coating. Silicon with respect to aluminium has a slower oxidation rate, as a consequence the current distribution and the oxide front are not propagating uniformly within the substrate. In particular, in the presence of large Si structures (greater than few μm), flaws such as unoxidized areas, cracks and gas-filled porosities are encountered [3]. Both the corrosion resistance and mechanical

properties are drastically reduced in the presence of a non-uniform oxide layer. On the opposite side, when silicon is finely dispersed inside the α-aluminium matrix, the oxide coating is not suffering from the abovementioned defects.

In the present work, an investigation aimed to mitigate the negative effects of Si on the anodizability of Al-Si alloys was conducted by using intense electron beam pulses. In particular, RITM-SP and SOLO units were employed. RIMT-SP allows for the pulsed electron beam treatment of conductive substrates with an energy density ranging from 1 to 6 J/cm^2 and an average pulse duration of 2.5 μs. This electron beam source works on a low accelerating voltage (10–30 kV) and a high-current (up to 30 kA) regime. It relies on an explosive-emission cathode and a plasma-filled diode where the beam is accelerated within the transport channel and guided by means of an external magnetic field [4–6]. SOLO allows for a dynamic power control along sub-millisecond (20–250 μs) pulses. The beam is developed from a plasma cathode with grid stabilization of the emission plasma boundary. In this way, the beam energy density reaches up to 100 J/cm^2 with electron accelerating voltage of 5–25 kV and beam current of 20–300 A [7–9].

Hao et al. conducted several studies on pulsed electron beam irradiation of eutectic [10] and hypereutectic [11–13] Al-Si alloys. Al-Si12.6 was treated at 3 J/cm^2 with 10 pulses of 1 μs average duration. A molten layer of about 10 μm was observed where the microstructure and the composition were homogenized. Effects on Al-Si15, Al-Si17.5 and Al-Si20 were also investigated at 2.5 J/cm^2 with 5, 15 and 25 pulses (0.1 Hz repetition frequency). The modified surface layer was composed by equiaxed grains of micrometric size. Moreover, the shift and the broadening of peaks in XRD spectra were associated to the formation a supersaturated solid solution of Al containing Si in higher content with respect to the equilibrium solubility. From a mechanical point of view, surface hardening and improved wear behavior were observed. This was mainly attributed by the authors to the formation of an Al-Si solid solution, to the dispersion of Si nanocrystals and to the presence of thermally induced residual stresses in the material.

Ivanov et al. investigated the modification of hypoeutectic Al-Si alloys with intense electron beams produced by SOLO equipment (20–35 J/cm^2, 150 μs, 3 pulses, 0.3 Hz). The treatment led to the dissolution of silicon inclusions and intermetallic compounds accompanied by the release of submicrometric second phase particles. Moreover, a drastic (2×) decrease of the silicon concentration in the remelted layer was detected [14]. According to Ustinov et al., the electron beam modified hypoeutectic Al-Si alloy is constituted by a fine dendritic structure up to 100 μm from the surface, with a remarkable increase in the plasticity of the material [15]. In the case of hypereutectic Al-Si alloys, modification of the surface layer was performed by Ashurova et al. by maintaining constant delivered energy density for 200 μs (20 J/cm^2) and then varying the holding time of temperature up to 800 μs. In this case the wear resistance of the material was found to be increased [16]. Fatigue life of Al-Si19 was prolonged by 3.5 times by Ivanov et al. [17], who investigated the effect of different energy densities, up to 25 J/cm^2, and different durations of the quasi-rectangular beams current pulse.

1. Materials and Methods

Samples were cut from cast ingots containing 7, 12 and 24% of silicon. They were mechanically polished (100, 320 and 600 grit), ultrasonically washed in 50 vol % acetone and 50 vol % ethanol for 15 minutes, rinsed in deionized water and dried with nitrogen. Metallographic etching was performed on pristine alloys to highlight the microstructure using Keller reagent with 5 second of immersion and rinsing in deionized water.

RITM-SP treatment was performed with electron accelerating voltage set at 20 and 25 kV, corresponding to the energy densities of 2.5 and 3.3 J/cm^2, respectively. Number of pulses were

2, 4, 8, 16 and 32, with pulse average duration of 2.5 μs and 0.2 Hz of repetition frequency. On the other hand, SOLO delivered energy density was fixed at 25 J/cm^2 with pulse number equal to 3, repetition frequency of 0.3 Hz and the average pulse duration of 200 μs.

Hard anodic oxidation was carried out in galvanostatic condition at 2 A/dm^2 inside a jacketed glass reactor containing 17.5% v/v H_2SO_4 (3.2 M) aqueous solution. Temperature was kept at 0 °C (± 1 °C) using a Julabo FP50 cryostat. A titanium mesh was employed as cathode with a 3:1 ratio between cathode and anode area. The distance between cathode and anode was 30 mm. Thickness of the oxide was measured by a Fisher Dualscope eddy-current probe.

Cross-sectional morphology was investigated using a Zeiss EVO 50VP SEM equipped with a Bruker Quantax X-ray spectrometer for EDS chemical microanalysis. The crystalline structure was characterized by X-ray diffraction in grazing incidence angle (GI-XRD) and Bragg-Brentano (BB) configuration using a PANalytical EMPYREAN PW1830 diffractometer. Surface hardness was assessed using a Fischer H100 Vickers microindenter. Potentiodynamic tests were performed using a AMEL 2049 potentiostat in 3.5% NaCl solution at room temperature. A three-electrode cell was employed with Al-Si sample as WE, a platinum mesh as CE and a saturated calomel electrode as REF. Open circuit potential was measured for 30 minutes with acquisition rate of 1 Hz. Then, a linear sweep voltammetry was performed from –250 mV to +250 mV with respect to OCP at a scan rate of 10 mV/min.

2. Results and discussion

Electron beam irradiation by means of RITM-SP and SOLO leads to rapid surface melting and solidification of Al-Si alloys inducing drastic modifications of surface morphology and composition. Fig. 1 shows a comparison between the mirror polished surface of Al-Si7 alloy and treated ones at 2.5 and 3.3 J/cm^2 with RITM-SP low-energy high-current electron beam. The characteristic microstructure of hypoeutectic Al-Si alloys can be recognized in the reference sample, in particular a clear distinction between the α-Al phase and the Si elongated grains of the eutectic structure is visible. After RITM-SP irradiation silicon features are not recognizable anymore, instead cracks and craters are observed. Craters are commonly found in LEHCEB (low energy high current electron beam) modified metals and they are originated by the ejection of impurities and second phases from the base material. This phenomenon is ascribed to the low thermal conductivity of such features that are overheated during the treatment, as a general rule their size and density decreases with the number of pulses, leading to a more homogeneous morphology. On the other hand, cracks can be originated during the rapid solidification shrinkage or due to the high thermally induced stresses.

Fig. 2 shows the XRD spectra of samples treated at 2.5 and 3.3 J/cm^2 with 16 and 32 pulses. After EB irradiation Si peaks decrease in intensity and almost completely disappear with respect to the pristine alloy, moreover an overall right shift of the α-Al phase peaks in observed. As a consequence, aluminium FCC cell parameter is decreased after electron beam surface treatment. This modification of the cell parameter can be linked to the formation of supersaturated solid solution between Al and Si, with a content of silicon higher that the equilibrium value, as reported by Hao et al. [12]. However, the presence of other alloying elements (Mg, Zn, Fe) and the remarkable lattice distortions caused by the EB treatment both play an important role in defining the lattice parameter of the aluminium phase and the different contributions are hardly decoupled clearly without further investigations. A reasonable hypothesis is that the eutectic Si grains originally present in the alloy are to some degree evaporated, dispersed in fine particles within Al matrix and brought in solid solution with Al.

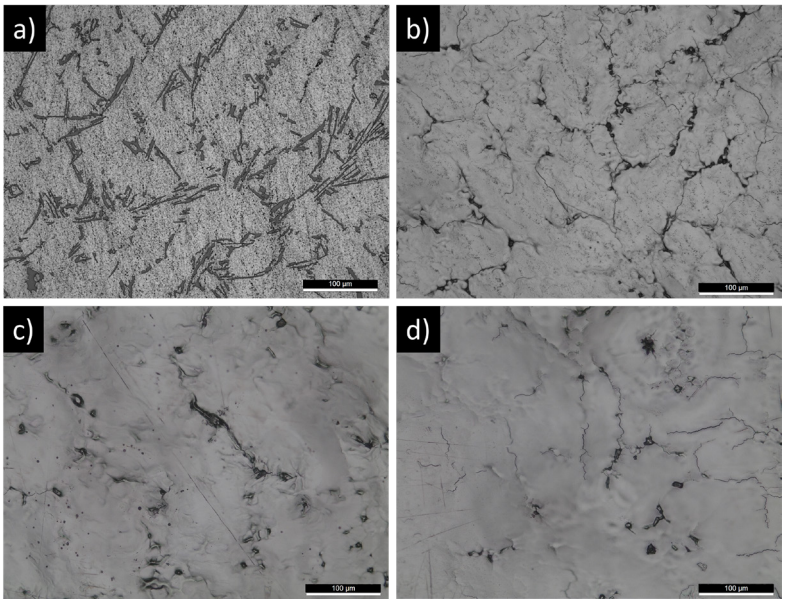

Fig. 1. Surface morphology (optical microscopy) of:
a) pristine Al-Si7; b) 2.5 J/cm² – 32 pulses; c) 3.3 J/cm² – 16 pulses and d) 3.3 J/cm² – 32 pulses

Рис. 1. Морфология поверхности (оптическая микроскопия):
a) исходный сплав Al-Si7; b) 2,5 Дж/см² – 32 импульса; c) 3,3 Дж/см² – 16 импульсов; d) 3,3 Дж/см² – 32 импульса

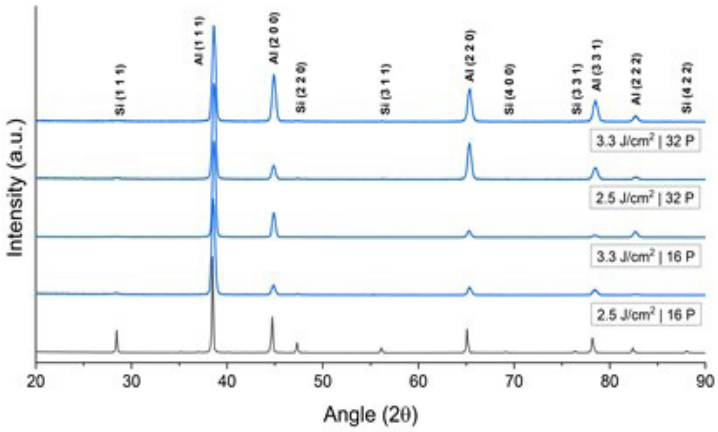

Fig. 2. Grazing Incidence XRD spectra of RITM- SP treated samples (black line pristine Al-Si7 alloy)

Рис. 2. Рентгенограммы образцов силумина Al-Si7 (съемка в геометрии скользящего пучка) после обработки на установке «РИТМ-СП» (черная линия – необработанный сплав)

SOLO treatment was carried out with fixed conditions (25 J/cm², 3 partially overlapped pules) on different alloys, namely Al-Si7, Al-Si12 and Al-Si24. Surface morphology of alloys before and after EB irradiation is reported in Fig. 3. Al-Si12 is characterized by large features of primary Al and by lamellar structures composed by the alternation of Al and Si, Al-Si24 instead shows massive primary Si grains embedded in a needle-like eutectic structure. SOLO irradiation was able to modify completely the surface morphology and texture of the alloys: in particular, a drastic increase of the surface roughness and a complete intermixing of Al and Si elements is observed. With respect to RITM-SP, the morphology of modified layers is less even and characterized by hills and valleys, on the other hand, few

craters and almost no cracks can be detected. SOLO and RITM-SP also differ concerning the penetration of the modified layer: the first one is able to melt and modify more than 20 μm at 25 J/cm^2 with 3 pulses, while the latter one around 5–10 μm at 2.5-3.3 J/cm^2 with 16 and 32 pulses. Fig. 4 shows XRD spectra of the three different alloys before and after SOLO irradiation: the intensity of silicon peaks is drastically reduced, even though they can be clearly identified in the case of Al-Si24. This suggests that silicon evaporation and dispersion in these alloys were less pronounced due to the very high content in the pristine material. On the treated samples, a right shift of the XRD peaks and consequently a decrease in the lattice parameter of Al phase was found.

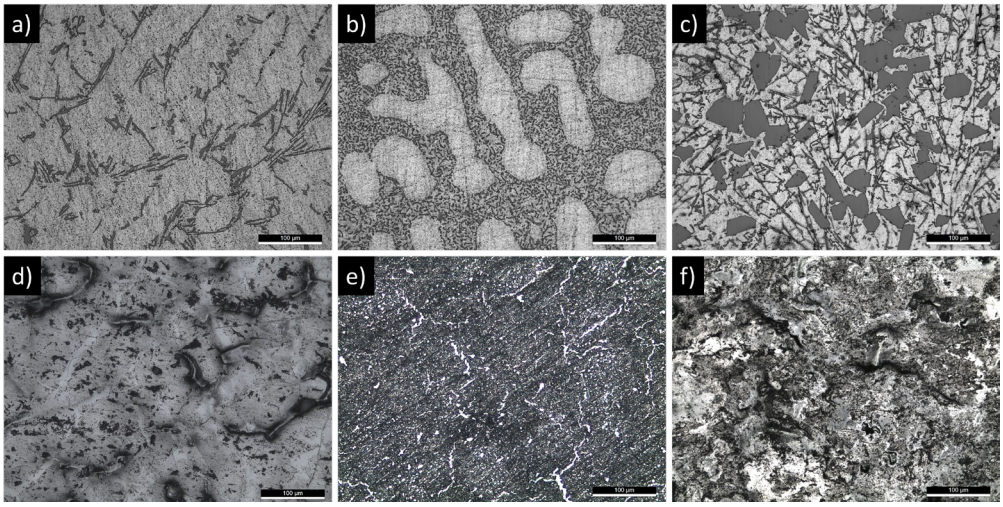

Fig. 3. Optical microscopy surface morphology of a) and d) Al-Si7, b) and e) Al-Si12, c) and f) Al-Si24 before and after SOLO surface modification at 25 J/cm^2

Рис. 3. Морфология поверхности (оптическая микроскопия): a) и d) Al-Si7, b) и e) Al-Si12, c) и f) Al-Si24 до и после модификации поверхности на установке «СОЛО» при 25 Дж/см^2

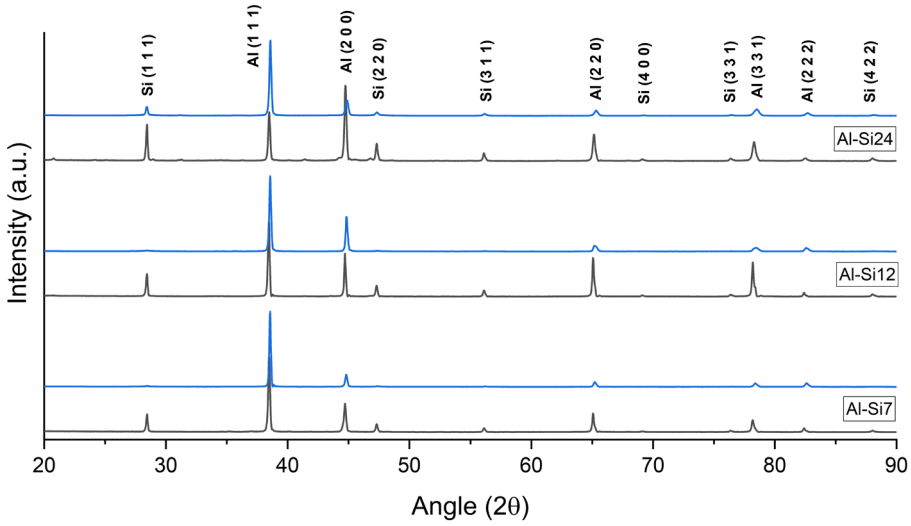

Fig. 4. Bragg Brentano XRD spectra of SOLO treated samples. Black lines refer to the as-cast Al-Si alloys while blue ones to the material modified by SOLO

Рис. 4. Спектры рентгеновской дифракции по схеме Брэгга-Брентано образцов после обработки на установке «СОЛО». Черными линиями обозначены сплавы системы Al-Si в литом состоянии, а голубыми – материалы, модифицированные на установке «СОЛО»

Anodic oxidation was performed on electron beam modified Al-Si alloys and average oxide thickness is reported it Table 1 for RITM-SP samples. After EB pre-treatment, the thickness of the anodic layer is slightly higher, even though the uncertainty in the measurement is increased as well, probably due to the higher surface roughness of the substrate on which the oxide is grown. Cell voltage was measured during the anodizing and the different curves are reported in Fig. 5. Pristine Al-Si alloy, displayed in black, shows a sharp increase of the voltage within the first seconds. During this stage, the growth of thin and compact layer of oxide is expected. Afterwards, a constant and slow increase in cell voltage is observed during which the thickness of anodic oxide is growing, making the whole substrate-coating system more and more resistive. Instead, RITM-SP pre-treated samples show a completely different voltage profile with respect to the pristine Al-Si7. The initial sharp step reaches higher voltages, followed by a constant and almost flat curve until the end of the process. This can be interpreted as a clear indication that the EB pre-treatment changes growth kinetics of the hard anodic oxide. It can be observed that there is no strict correlation between plateau voltage or final voltage and thickness of the oxide, neither can be found a link between the applied energy density or number of pulses and voltage profiles.

Table 1. Average anodic oxide thickness of RITM-SP pre-treated Al-Si7 alloy at different energy densities and number of pulses in comparison with the pristine material

Таблица 1. Средняя толщина анодно-осидных покрытий на сплаве Al-Si7, подвергнутом предварительной обработке на установке «РИТМ-СП» при различных плотностях энергии и числе импульсов, в сравнении с необработанным материалом

	Al-Si7 Ref	2.5 J/cm^2 | 16 P	3.3 J/cm^2 | 16 P	2.5 J/cm^2 | 32 P	3.3 J/cm^2 | 32 P
Thickness (μm)	23.05	24.04	25.12	22.83	25.19
Sigma (μm)	0.659	4.57	2.49	2.34	3.93

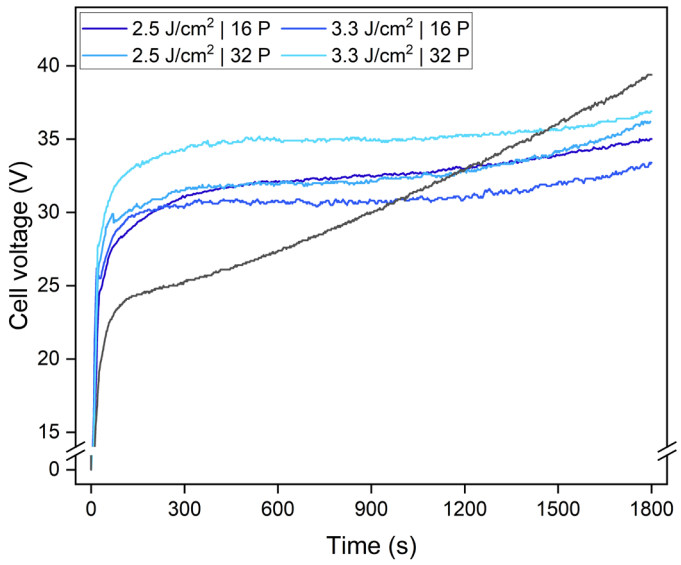

Fig. 5. Anodizing voltage profiles of RITM-SP pre-treated Al-Si7 alloy at different energy densities and number of pulses in comparison with the pristine material

Рис. 5. Профили напряжения при анодировании сплава Al-Si7, подвергнутого предварительной обработке на установке «РИТМ-СП» при различных плотностях энергии и числе импульсов, в сравнении с необработанным материалом

Fig. 6 shows the comparison between cross-sections of a pristine Al-Si7 oxide and two RITM-SP modified alloys togheter with their EDX elemental distribution maps. In picture a) the characteristic microstrucure of hypoeutectic Al-Si alloys can be recognized. The oxide layer in this case is highly inhomogeneous and characterized by porosities, cracks and unoxidized areas. As expected, large Si segregations are affecting the overall quality of the coating. Instead, oxide formed on pre-treated alloys is drastically different: the anodic layer is compact, homogenous and does not present visible defects. The main difference between samples shown in images b) (3.3 J/cm^2, 16 pulses) and c) (3.3 J/cm^2, 32 pulses) relies on the thickness of the EB modified layer. A small portion of the oxide presented in image b) in fact still presents some hints of defects close to the interface with the metal substrate. This does not hold true in image c) where the coating is grown fully within the molten and rapidly solidified layer. In conclusion, RITM-SP pretreatment proved to be effective in modifying the substrate materials to produce a fine dispersion of Si which is not affecting the homogeneity of the anodic oxide.

Potentiodynamic polarization and microindentation measurements were done to characterize corrosion behaviour and mechanical resistance of the anodic oxides and results are reported in Fig. 7 and 8. The RITM-SP modification brought improvements in all tested operating conditions. In particular, corrosion current density was decreased down to $3.02 \cdot 10^{-7}$A/cm^2 (–83.5%) and Vickers microhardness was increased up to 320.62 HV (+46.5%). The lowest current density and highest hardness do not belong to the same sample, in fact the highest corrosion resistance is found at 2.5 J/cm^2 and 32 pulses, while the highest microhardness is found at 3.3 J/cm^2 and 32 pulses. In absolute terms the performance of the anodic oxides synthesized in the present work are slightly below average [18]. However, the aim was not to grow excessively thick coatings, but to appreciate as much as possible the effects of EB pretreatment. Future works will be devoted to filling this gap.

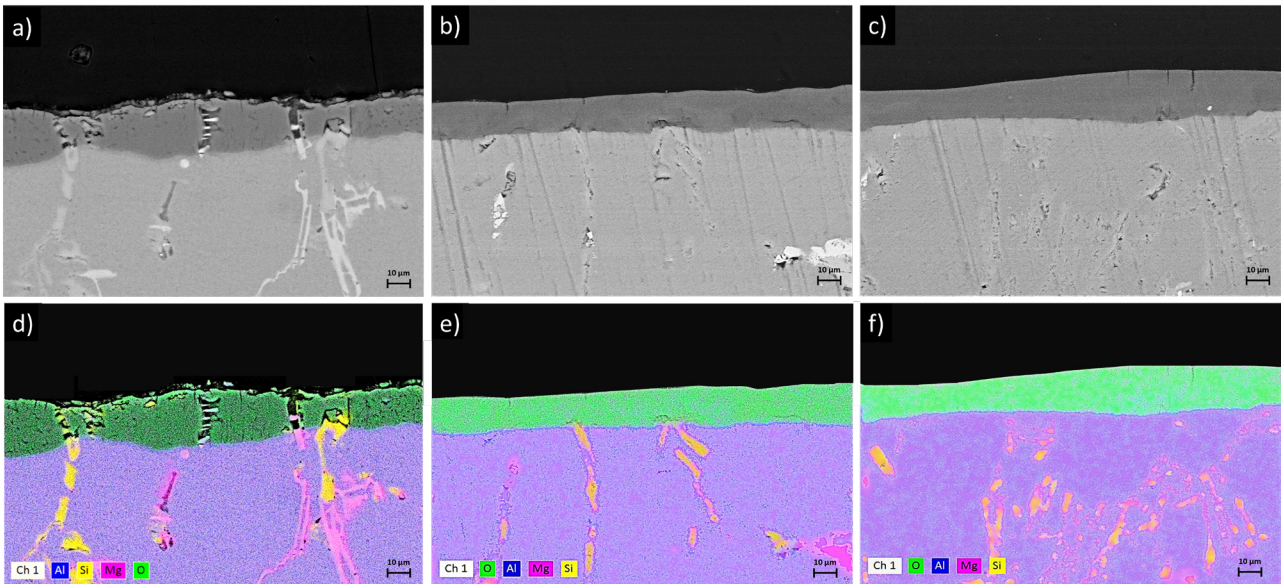

Fig. 6. SEM cross sections and EDS elemental maps of a), d) pristine Al-Si7 anodized alloy, b), e) and c), f) RITM-SP pretreated and anodized alloy at 3.3 J/cm^2 at 16 and 32 pulses, respectively

Рис. 6. РЭМ-изображения поперечного сечения и элементное картирование, полученное методом ЭДС: a), d) необработанный сплав Al-Si7 после анодирования, b), e) и c), f) сплав, подвергнутый предварительной обработке на установке «РИТМ-СП» и анодированию при 3,3 Дж/см^2 при 16 и 32 импульсах соответственно

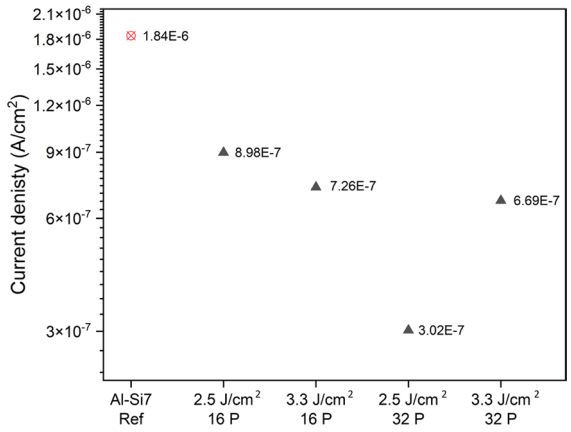

Fig. 7. Corrosion current density of anodic oxides comparing the effect of different pretreatment conditions with respect to the untreated substrate

Рис. 7. Плотность тока коррозии анодных оксидов; показано влияние различных условий предварительной обработки в сравнении с необработанной подложкой

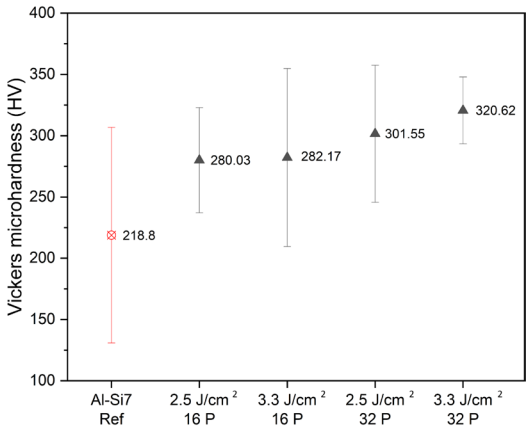

Fig. 8. Vickers microhardness of anodic oxides comparing the effect of different pretreatment conditions with respect to the untreated substrate

Рис. 8. Микротвердость по Виккерсу анодных оксидов; показано влияние различных условий предварительной обработки в сравнении с необработанной подложкой

Table 2 shows average thickness of oxides comparing the untreated Al-Si substrates and the SOLO pretreated materials at 25 J/cm^2. After EB irradiation, the anodic layer is on average thicker with respect to that of the as cast substrates. Moreover, SOLO Al-Si7 oxide has a higher thickness compared with RITM-SP pretreated material, both at 2.5 and 3.3 J/cm^2. This difference is probably related to the higher modified depth reached by SOLO and by the different chemical composition and microstrucure obtained after the two electron beams. The largest difference is found for Al-Si24 alloy. On the pristine material oxide was barely grown while after irradiation an anodic layer of 16.7±6.9 μm was obtained. This peculiar result allows us to conclude that EB surface treatment can be effectively employed to allow not anodizable alloys (*i.e.* highly hypereutectic ones) to be coated by means of hard anodic oxidation. Fig. 9 shows the measured cell voltage during oxidation of pristine and modified alloys. Al-Si7 does not show a drastic modification of the voltage profile, as observed with RITM-SP, and simply shows a faster increase with respect to the untreated material up to a higher final voltage. In the case of Al-Si12 a much higher slope of the voltage profile was measured and, as a consequence, the upper limit of the power supply was reached after about 1200 s (identified in the plot with the dashed line). Pristine Al-Si24 showed a flat and constant voltage profile around 7 V and, as anticipated, was barely anodized. Moreover, a large oxygen evolution close to the anodic surface was observed. Instead, after SOLO irradiation, a different voltage profile was found, confirming a drastic change induced by the EB pretreatment in the base material.

Table 2. Average anodic oxide thickness of SOLO pretreated Al-Si alloys at 25 J/cm^2 in comparison with the pristine materials

Таблица 2. Средняя толщина анодно-оксидных покрытий на сплавах системы Al-Si, подвергнутых предварительной обработке на установке «СОЛО» при 25 Дж/см^2, в сравнении с необработанными материалами

	Ref thickness (μm)	Sigma (μm)	SOLO thickness (μm)	Sigma (μm)
Al-Si7	25.11	0.758	30.18	3.02
Al-Si12	27.13	3.01	32.82	5.69
Al-Si24	4.41	0.663	16.74	6.91

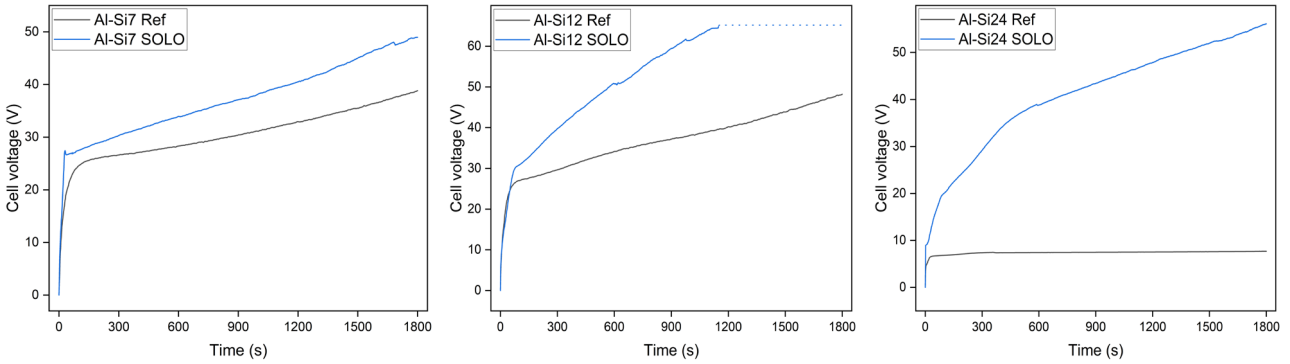

Fig. 9. Anodizing voltage profiles of pristine and SOLO pretreated Al-Si alloys at 25 J/cm^2

Рис. 9. Профили напряжения при анодировании сплавов системы Al-Si в необработанном состоянии и после предварительной обработки на установке «СОЛО» при 25 Дж/см^2

Fig. 10 shows SEM cross-sections of anodized reference Al-Si alloys and anodized SOLO modified substrates. Anodic layers grown on pristine Al-Si7 and Al-Si12 alloys present the expected defects ascribed to the presence of coarse Si structures. In all the pretreated samples, slightly below the interface between oxide and metal, a 10–20 μm thick layer formed by SOLO modification can be observed. The cross-sectional morphology and microstructure appear to be different with respect to the pristine alloys: eutectic structure, segregations and second phases are molten by the electron irradiation and completely intermixed with the Al matrix, leading to a homogenous and free-of-defect material from which the anodic oxide is formed. The highest difference can be seen in the Al-Si24 sample, which is the one characterized by the largest disuniformities in the pristine condition, as showed in Fig. 3. Concerning the oxide layer, SOLO pretreated Al-Si7 in comparison to the RITM-SP one shows a slightly lower regularity in thickness and the presence of small cracks. The comparison in this case is also drastically in favour of the pretreated alloy in terms of absence of defects (cracks, porosities and unoxidized Si particles) and in terms of uniformity. The same conclusions can be drawn for the Al-Si12 alloy. Moreover, oxide formed on as-cast Al-Si12 suffers from drastic variations of thickness due to the alternation of large Al-rich areas, where the coating grows quickly, and Si-rich areas, where the coating grows rich in flaws and slowly. This effect is not observed anymore after SOLO irradiation of the substrate, confirming the beneficial effects of EB pretreatment of Al-Si alloys before hard anodic oxidation. Lastly, on the cross-section of the reference Al-Si24, it is barely possible to appreciate the presence of an oxide (which is measured to be around 3 μm on average), while on the modified alloy a dense and thick anodic layer is observed, with only few microcracks.

EDS qualitative line profiles and quantitative pointwise analyses were performed, in order to characterize the elemental composition of the anodic oxides. Line profiles are reported in Fig. 11, while pointwise compositions in Table 3. Aluminium and oxygen signals can be used to confirm the thickness of anodic layer from a chemical point of view, while silicon signal is exploited to investigate the effect of SOLO irradiation on the substrate and on the oxide. Considering the pristine Al-Si alloys, silicon counts within the coating are low and close the background, except when a Si particle is encountered. Instead, after EB modification, within the oxide a non-negligible intensity of silicon signal is found. The homogenous silicon dispersion and the hypothesized Al-Si supersaturated solid solution formed during EB irradiation are incorporated in the oxide, probably resulting in the synthesis of a mixture of Al and Si oxide. This hypothesis is supported by the pointwise elemental analysis, which was repeated three times to guarantee accuracy of the measurements. Silicon contents in the pristine oxide, always measured in less defective area,

were 0.40 and 0.67% for Al-Si7 and Al-Si12, respectively. After SOLO pretreatment, the values increased to 2.65 and 9.86%. Silicon content inside modified Al-Si24 was 9.02% but without reference measurement due to the insufficient thickness of pristine oxide. Further investigations are required to clarify whether Si and Al formed a mixed oxide or Si-oxide is finely and uniformly embedded inside Al-oxide. Mass balance to reach 100% is composed of sulphur, incorporated from the electrolyte, and other minor alloying elements such as Zn and Fe in very low content and not present in all the alloys.

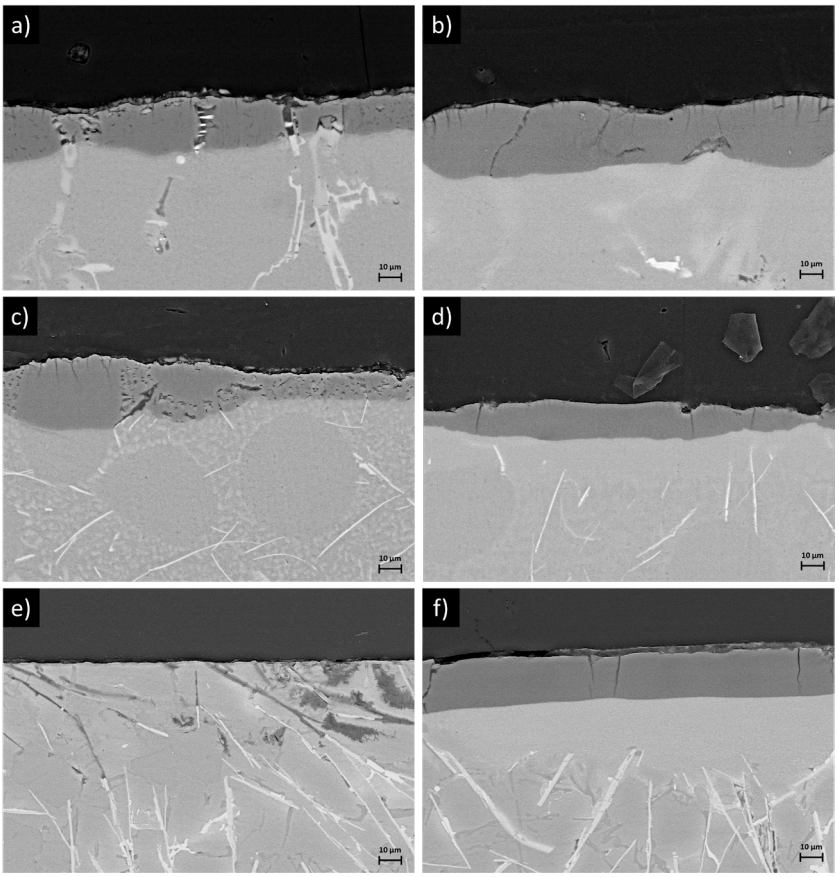

Fig. 10. SEM cross-sections of pristine a) Al-Si7, c) Al-Si12, e) Al-Si24 anodized alloys and SOLO pretreated at 25 J/cm^2 b) Al-Si7, d) Al-Si12, f) Al-Si24 anodized alloys

Рис. 10. РЭМ-изображения поперечного сечения необработанных сплавов: a) Al-Si7, c) Al-Si12, e) Al-Si24 после анодирования и сплавов, подвергнутых предварительной обработке на установке «СОЛО» при 25 Дж/см^2: b) Al-Si7, d) Al-Si12, f) Al-Si24 после анодирования

Table 3. EDS quantitative pointwise elemental analysis of pristine and SOLO pre-treated Al-Si alloys

Таблица 3. Количественный поточечный элементный анализ с помощью ЭДС необработанных и подвергнутых предварительной обработке на установке «СОЛО» сплавов системы Al-Si

	Oxygen %	Aluminium %	Silicon %	Magnesium %
Al-Si7 Ref	45.55	46.45	0.40	0.16
Al-Si7 SOLO	45.57	44.43	2.65	0.27
Al-Si12 Ref	39.39	52.56	0.67	0.11
Al-Si12 SOLO	41.24	41.61	9.86	0.12
Al-Si24 Ref	/	/	/	/
Al-Si24 SOLO	43.53	39.58	9.02	0.00

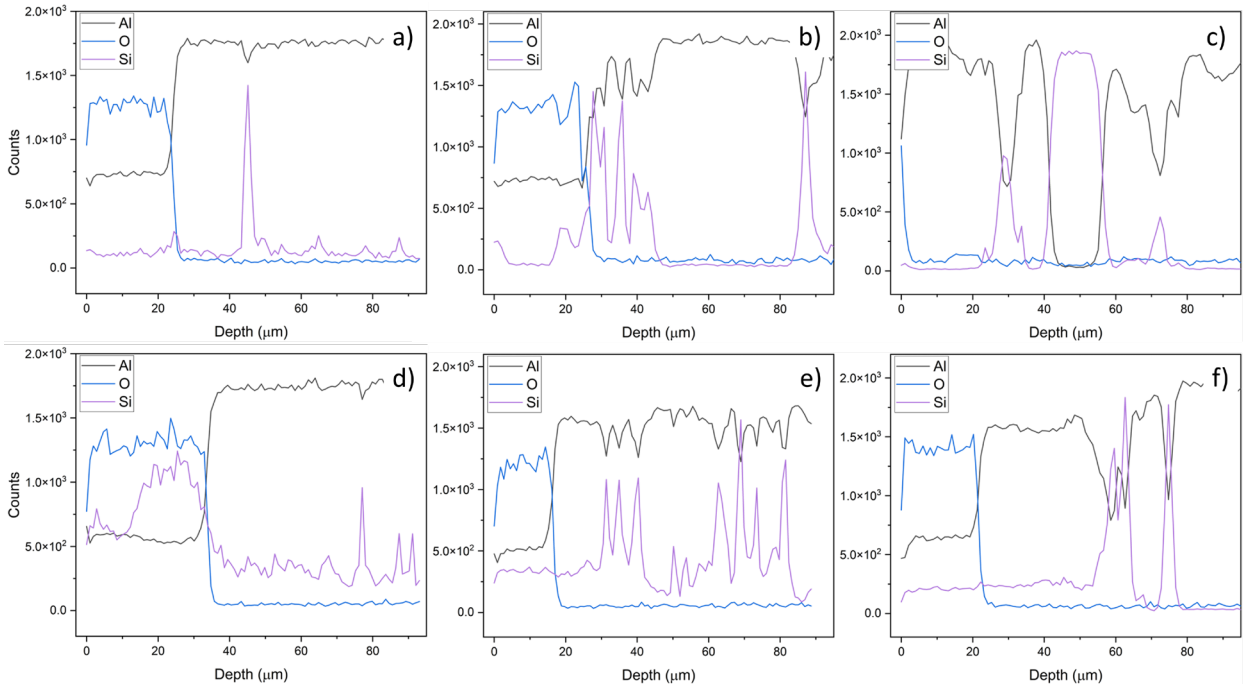

Fig. 11. EDS qualitative elemental line profiles for of pristine a) Al-Si7, b) Al-Si12, c) Al-Si24 anodized alloys and SOLO pre-treated at 25 J/cm^2 d) Al-Si7, e) Al-Si12, f) Al-Si24 anodized alloys

Рис. 11. Качественные профили линий элементов, полученные с помощью ЭДС, для необработанных сплавов: a) Al-Si7, b) Al-Si12, c) Al-Si24 после анодирования и сплавов, подвергнутых предварительной обработке на установке «СОЛО» при 25 Дж/см^2: d) Al-Si7, e) Al-Si12, f) Al-Si24 после анодирования

Reference and modified oxides were characterized in term of corrosion resistance and surface hardness, results are displayed respectively in Figs. 12 and 13. The three Al-Si alloys showed different corrosion current densities and Vickers microhardness both before and after EB irradiation, without a clear trend between the content of silicon and the measured surface properties. SOLO pretreatment, as for RITM-SP, brought positive outcomes in all the tested conditions. Corrosion current density and microhardness of Al-Si7 are in line with values obtained after the RITM-SP irradiation. Pretreated Al-Si7 oxide showed the highest microhardness among SOLO samples. Instead, the increase in microhardness of Al-Si12 was probably partially hindered by the presence of microcracks, which weakened the anodic layer. The greatest increase in hardness was observed for Al-Si24. However, measurements on Al-Si24 oxide formed on the pristine substrate should be ascribed to the bare substrate and not to any protective coating, since the very low thickness and uneven coverage of the oxide gave a negligible contribution. The anodic oxide on the untreated Al-Si12 showed the lowest current density and the highest increase in corrosion resistance in comparison with treated Al-Si7 and Al-Si24. The very low corrosion resistance of the anodic layer formed on pretreated Al-Si24 should be related to poor or nonuniform growth of the oxide, since a dense and homogenous coating was observed in the SEM magnified area. The thicknesses of all the oxides formed on SOLO pretreated alloys are lower than the depths modified by electron beam irradiation, in contrast with RITM-SP tested conditions. For this reason, a thicker anodic coating could be realized in combination with SOLO surface modification to improve even further the beneficial effects found in the present work.

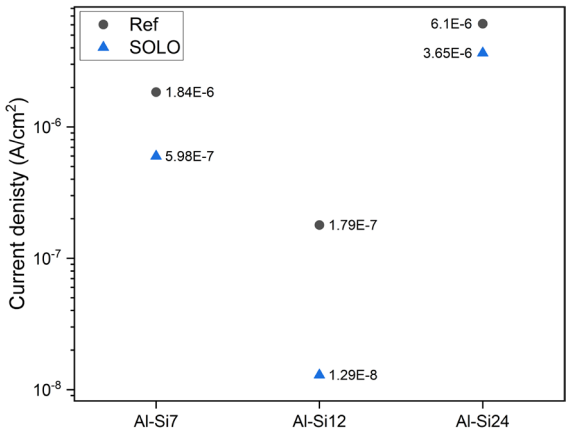

Fig. 12. Corrosion current density of different Al-Si alloy oxides pre-treated with SOLO at 25 J/cm^2 with respect to the untreated substrates

Рис. 12. Плотность тока коррозии оксидов на поверхности различных сплавов системы Al-Si, подвергнутых предварительной обработке на установке «СОЛО» при 25 Дж/см^2, по сравнению с необработанными подложками

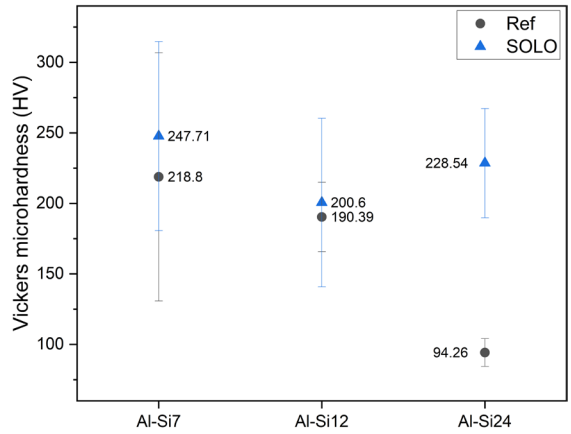

Fig. 13. Vickers microhardness of different Al-Si alloy oxides pre-treated with SOLO at 25 J/cm^2 with respect to the untreated substrates

Рис. 13. Микротвердость по Виккерсу оксидов на поверхности различных сплавов системы Al-Si, подвергнутых предварительной обработке на установке «СОЛО» при 25 Дж/см^2, по сравнению с необработанными подложками

Conclusions

In the present work, RITM-SP and SOLO pulsed electron beams were employed to induce surface modifications on Al-Si7, Al-Si12 and Al-Si24. The aim was to disperse and homogenize coarse Si structures and other second phases in order to increase anodizability of the alloys. The compositional, morphological and microstructural characterization of modified Al-Si alloys allowed us to conclude that silicon was partially evaporated during irradiation, finely dispersed in small particles and likely brought in solid solution with aluminium. RITM-SP irradiation led to a smoother and more homogeneous surface morphology, while SOLO was able to induce a deeper modification up to 20–30 μm. Hard anodic oxidation was performed and the influence of EB pretreatments was investigated by potentiodynamic polarization and microindentation measurements. RITM-SP modification on Al-Si7 alloy led to a compact, homogenous and flawless anodic oxide, with higher corrosion resistance and surface microhardness. SOLO modification on Al-Si7, Al-Si12 and Al-Si24 brought similar positive results with respect to the prior treatment concerning hypoeutectic and eutectic alloys. The hypereutectic alloy, which was not even barely anodized in the pristine condition, was strongly EB modified allowing the formation of a thick and hard anodic layer. In conclusion, surface modification induced by pulsed intense electron beams effectively prepared a micrometric surface layer for hard anodic oxidation allowing to obtain a protective coating with higher corrosion resistance and higher microhardness.

REFERENCES

1. Fratila Apachitei L. E., Duszczyk J., Katgerman L. Vickers microhardness of AlSi (Cu) anodic oxide layers formed in H2SO4 at low temperature // Surface and Coatings Technology. 2003. V. 165, Iss. 3. P. 309–315. DOI: 10.1016/S0257-8972(02)00750-8.

2. Fratila Apachitei L. E., Terryn H., Skeldon P., Thompson G. E., Duszczyk J., Katgerman L. Influence of substrate microstructure on the growth of anodic oxide layers // Electrochimica Acta. 2004. V. 49, Iss. 7. P. 1127–1140. DOI: 10.1016/j.electacta.2003.10.024.

3. Scampone, G., Timelli G. Anodizing Al-Si foundry alloys: A critical review // Advanced Engineering Materials. 2022. V. 24, Iss. 4. Article number 2101480. DOI: 10.1002/adem.202101480.

4. Proskurovsky D. I., Rotshtein V. P., Ozur G. E., Ivanov Yu. F., Markov A. B. Physical foundations for surface treatment of materials with low energy, high current electron beams // Surface and Coatings Technology. 2000. V. 125, Iss. 1–3. P. 49–56. DOI: 10.1016/S0257-8972(99)00604-0.

5. Rotshtein V., Ivanov Yu., Markov A. Surface treatment of materials with low-energy, high-current electron beams // Materials surface processing by directed energy techniques. 2006. V. 6. P. 205–240. DOI: 10.1016/B978-008044496-3/50007-1.

6. Ozur G. E., Proskurovsky D. I., Rotshtein V. P., Markov A. Production and application of low-energy, high-current electron beams // Laser and Particle Beams. 2003. V. 21, Iss. 2. P. 157–174. DOI: 10.1017/S0263034603212040.

7. Koval N. N. New electron-ion-plasma equipment for modification of materials and products surface // Interaction of radiation with solids. Proc. 10th international conference (Belarus), 2013. P. 384.

8. Vorobyov M. S., Moskvin P. V., Shin V. I., Koval N. N., Ashurova K. T., Doroshkevich S. Yu., Devyatkov V. N., Torba M. S., Levanisov V. A. Dynamic power control of a sub millisecond pulsed megawatt electron beam in a source with a plasma cathode // Technical Physics Letters. 2021. V. 47. P. 528–531. DOI: 10.1134/S1063785021050291.

9. Devyatkov V. N., Koval N. N. Pulsed electron source with grid plasma cathode and longitudinal magnetic field for modification of material and product surfaces // Russian Physics Journal. 2018. V. 60. P. 1509–1514. DOI: 10.1007/s11182-018-1243-7.

10. Hao Y., Gao B., Tu G. F., Cao H., Hao S. Z., Dong C. Surface modification of Al-12.6 Si alloy by high current pulsed electron beam // Applied Surface Science. 2012. V. 258, Iss. 6. P. 2052–2056. DOI: 10.1016/j.apsusc.2011.04.104.

11. Hao Y., Gao B., Tu G. F., Li S. W., Dong C., Zhang Z. G. Improved wear resistance of Al-15Si alloy with a high current pulsed electron beam treatment // Nuclear Instruments and Methods in Physics Research Section B: Beam Interactions with Materials and Atoms. 2011. V. 269, Iss. 13. P. 1499–1505. DOI: 10.1016/j.nimb.2011.04.010.

12. Hao Y., Gao B., Tu G. F., Wang Z., Hao Sh. Zh. Influence of high current pulsed electron beam (HCPEB) treatment on wear resistance of hypereutectic Al-17.5 Si and Al-20Si alloys // Materials Science Forum. 2011. V. 675–677. P. 693–696. DOI: 10.4028/www.scientific.net/MSF.675-677.693.

13. Hao Y., Gao B., Tu G. F., Li S. W., Hao S. Z., Dong C. Surface modification of Al-20Si alloy by high current pulsed electron beam // Applied Surface Science. 2011. V. 257, Iss. 9. P. 3913–3919. DOI: 10.1016/j.apsusc.2010.11.118.

14. Ivanov Yu. F., Gromov V. E., Konovalov S., Zagulyaev D. V., Petrikova E. A., Semin A. P. Modification of structure and surface properties of hypoeutectic silumin by intense pulse electron beams // Progress in Physics of Metals. 2018. V. 19, Iss. 2. P. 195–222. DOI: 10.15407/ufm.19.02.195.

15. Ustinov A., Klopotov A. A., Ivanov Yu., Zagulyaev D. V., Teresov A., Petrikova E., Gurianov D. A., Chumaevskii A. V. Deformation inhomogeneities of a hypoeutectic aluminum-silicon alloy modified by electron beam treatment // Materials. 2023. V. 16, Iss. 6. Article number 2329. DOI: 10.3390/ma16062329.

16. Ashurova, K. T., Vorobyov M. S., Petrikova E. A., Ivanov Yu. F., Moskvin P. V., Rygina M. E. Surface modification of hypereutectic silumin subjected to a millisecond modulated electron beam treatment // Journal of Physics: Conference Series. 2021. V. 2064, Iss. 1. Article number 012045. DOI: 10.1088/1742-6596/2064/1/012045.

17. Ivanov Yu. F., Alsaraeva K., Gromov V., Konovalov S., Semina O. Evolution of Al–19· 4Si alloy surface structure after electron beam treatment and high cycle fatigue // Materials science and technology. 2015. V. 31, Iss. 13. P. 1523–1529.

18. Li X., Nie X., Wang L., Northwood D. O. Corrosion protection properties of anodic oxide coatings on an Al-Si alloy // Surface and Coatings Technology. 2005. V. 200, Iss. 5–6. P. 1994–2000. DOI: 10.1016/j.surfcoat.2005.08.019.